applied mechanics

MDPI

Article

Response Surface Methodology (RSM)-Based Evaluation of the 3D-Printed Recycled-PETG Tensile Strength

Lazaros Firtikiadis *, Anastasios Tzotzis *, Panagiotis Kyratsis and Nikolaos Efkolidis

Department of Product and Systems Design Engineering, University of Western Macedonia, Campus Kila Kozani, GR50100 Kozani, Greece; pkyratsis@uowm.gr (P.K.); nefkolidis@uowm.gr (N.E.)
* Correspondence: l.firtikiadis@uowm.gr (L.F.); a.tzotzis@uowm.gr (A.T.)

Abstract: In this research, an investigation related to the tensile testing of 3D-printed specimens, under different fabrication parameters, is presented. The control samples were fabricated using Recycled-PETG: EVO (NEEMA3D™, Athens, Greece). It consists of recycled polyethylene terephthalate glycol (PETG) raw material, already used in industry, modified so that it becomes filament and can be printed again. More specifically, the parameters set to be studied are the percentage of infill, the speed and the type of infill. Both infill density and printing speed have three value levels, whereas for the infill pattern, two types were selected. Two sets of 18 specimens each were fabricated, with respect to the different parameter combinations. Through the results of the tests, the maximum tension of each specimen was obtained separately. Of the three parameters defined, it was found that the most important are the type of infill (44.77%) and the percentage of infill (24.67%). Speed (13.22%) did not strongly affect the strength of the specimens. In conclusion, the empirical model developed was considered reliable in terms of the value of the squared error, R-sq(pred) (97.72%), but also of the rest of the resulting analysis residual graphs (through the full factorial design).

Keywords: additive manufacturing; polyethylene terephthalate glycol recycling; PETG-r; tensile tests; analysis

Citation: Firtikiadis, L.; Tzotzis, A.; Kyratsis, P.; Efkolidis, N. Response Surface Methodology (RSM)-Based Evaluation of the 3D-Printed Recycled-PETG Tensile Strength. *Appl. Mech.* **2024**, *5*, 924–937. https://doi.org/10.3390/applmech5040051

Received: 31 October 2024
Revised: 29 November 2024
Accepted: 2 December 2024
Published: 4 December 2024

1. Introduction

Nowadays, fused deposition modeling (FDM) is being widely used in several industries. The production of additives through the continuous layering of molten material provides the possibility to obtain special structures at a relatively low cost and in a short period of time. This particular 3D printing technology is an important subject of study for the thermal and mechanical properties of synthetic materials used in additive manufacturing. The studies carried out focus on various materials, but mainly on Acrylonitrile butadiene styrene (ABS), Polylactic acid (PLA) and Thermoplastic Polyurethane (TPU), which are also the most popular on the market [1–3]. However, the need that has arisen to reduce waste pollution and strengthen the circular economy leads to a new trend: the use of recycled polymers from plastic objects in the form of thread for 3D printing (PLA-r, ABS-r) [4–7]. An additional thermoplastic elastomer now appearing in 3D printing filaments is polyethylene terephthalate glycol (PETG). For this material, it is found that the improvement of its properties, but mainly of the recycled material, is a promising research topic for a wider and more effective application.

Most of the studies described below focused on testing the mechanical properties for PETG material and its recyclability. Tensile, bending and compression test methods were applied, individually or in combination. At the same time, in order to achieve the correct control and validity of the studies, the tests used are based on ASTM and ISO standards [8,9]. Özen et al. used control specimens to study the mechanical properties of PETG. Standards were selected to define the characteristics of the specific material used as a filament in fused deposition modeling (FDM). This particular research was based on

two directions of study. First, in digital control through the finite element method (FEM) and then through the tensile method in the 3D-printed samples [10]. Hanon et al. defined specific parameters in 3D-printed samples in order to test the mechanical properties of polyethylene terephthalate glycol (PETG). The parameters selected were for five different patterns and infill percentage, raster direction angles and print orientation in all three axes, X, Y, Z. Through the tensile test method, the corresponding diagrams that led to the conclusions of the study were also obtained [11]. To analyze the data obtained from the tensile strength, deformation, Young's modulus and yield stress through the test specimens, Minitab^{TM} software is used [12].

After the implementation of different methodologies and analyses, the appropriate use of recycled PETG as a 3D printing filament is established. Properties identical to those of commerce make it a solution that will contribute to the improvement of the life cycle of polymers in the industry [13–15]. Flores et al. dealt with the recycling of PETG polymer material to create a filament suitable for 3D printing with the FFF (material deposition) technology. The possibility of processing the specific material allowed five recycling cycles. According to the studies carried out it was found that the mechanical properties of recycled PETG can be compared to those of commercially available printing filaments. The above process can be an alternative solution for the recycling and reuse of polymers [16]. Vidakis et al. dealt with the recycling of PETG. The control of its properties in continuous recycling processes was performed through methods of tensile strength, impact resistance, bending and Vickers microhardness. In addition, a series of thermal and morphological analyses were carried out. All this contributed to the conclusion that PETG, even if it loses its mechanical properties to a small extent, can be used as a recyclable material in 3D printing [17]. Lehrer and Scanlon studied the mechanical properties of recycled polyethylene terephthalate (PET) yarn. Its goal is to highlight recycled yarns as sustainable materials that can be used in fused deposition modeling [18,19]. Mattew et al. focused on the influence that multiple recycling cycles of polymer composites have on their mechanical properties, as well as their energy performance. More specifically, these are materials used in fused deposition modeling (FDM). The test methods performed were tensile strength, carbon emission and energy consumption in different recycling cycles. The results of the research showed that recycled polymers can maintain their above properties at high levels, contributing in their own way positively to sustainability [20]. Latko-Durałek et al. reused poly(ethylene terephthalate) modified with glycol in order to create recycled PETG. The specific recycled PETG was formed on the basis of homogeneous mixtures, depending on the percentage of virgin PETG content they contained. The measurements carried out proved that the mechanical tensile strength and modulus of elasticity of the resulting materials are lower than those of virgin PETG. At the same time, the greater the amount of PETG, the greater the elongation at break of the specimens during the tensile test [21].

In addition to the comparisons between pure PETG and its recycled counterpart, their comparisons with other popular materials (PLA, ABS, Polystyrene (PS), Acrylonitrile styrene acrylate (ASA)) used in 3D printing are also a subject of study. Through tensile, bending and compression control methods, results are obtained from the parameters and printing conditions defined each time, with the ultimate goal of applying them to improved components in industry [22–25]. Kumar et al. highlighted the need to utilize the used 3D printing filaments, adding/bringing an ecological character to the industry. It was therefore deemed necessary to study the environmental effects of known materials (PETG, PLA and ABS), with the ultimate goal of choosing the most environmentally friendly material [26].

Thanks to the ecological character of the composite materials based on rPET, but also to the enhanced mechanical properties they present, their use as 3D printing materials has been established. The reinforcing materials chosen for this reason vary, from natural and synthetic fibers, mixed with various virgin polymers or even microfillers [27,28]. The most common and valid methods used to test mechanical properties for virgin and recycled materials (PETG) are tensile and fracture. The results through these methods certify the

possibility of using filament for 3D printing [29]. Additional studies wanted to establish whether recycled PETG has the potential to be used as a basic material for 3D printing, while containing carbon fibers. In a first phase, a comparison was made between virgin PETG and its recycled material, which also contained carbon fibers. In subsequent steps of the research, tensile and bending tests and SEM microscope studies of the results were carried out. In conclusion, PETG containing synthetic materials (CCF) can be used as a 3D printing material, while recyclable materials can contribute to the circular economy [30–32].

Considering the above literature and other research studies, a trend has been observed in the control of materials used in 3D printing. PETG is a widely studied material since it provides superior mechanical properties and constitutes an excellent matrix material for polymeric composites. In contrast, limited data are available for the recycled version of PETG and especially on its tensile properties, which are considered the most important mechanical parameters of a material. In addition, this study aims to combine structural characteristics such as the infill density and pattern with the critical printing parameter of speed. For this reason, this particular study aims at the investigation of the tensile strength of 3D-printed samples, with three basic 3D printing parameters. The material of the samples is Recycled-PETG: EVO (NEEMA3D™, Athens, Greece), recyclable polyethylene terephthalate glycol. The three parameters concerning the 3D printing settings are the percentage of infill (infill), the speed (speed) and the type of infill (type) [33]. Eighteen different experimental trials resulted from the full factorial design, with all possible combinations of these structural features. Finally, the empirical/mathematical model for each combination of values was defined through the aggregation and processing of the total stress results collected from the tensile test.

2. Materials and Methods

Experimental Setup

This work focuses on the mechanical strength of samples that were manufactured by utilizing a 3D printer. The parameters set/selected for the tests created a set of samples with different values under specific printing conditions. The testing of these samples was performed through a tensile machine and the measurement values were appropriately organized in tables. Then, using these values, diagrams were produced that depicted which parameters contributed the most to the strength. In order to derive an empirical formula that will be able to predict the strength of the specimens, within the specific range of all the values that the parameters could have, the response surface methodology (RSM) was applied [34–36]. Figure 1 shows schematically the stages of the entire study. It started from the printing of the samples with the specific values of the parameters in the first step, then in the second step their organization and categorization. In the third step, the testing of the samples was carried out in a tensile machine. Finally, in the fourth step, the analysis of the controls and the conclusions obtained from them are presented in an organized manner.

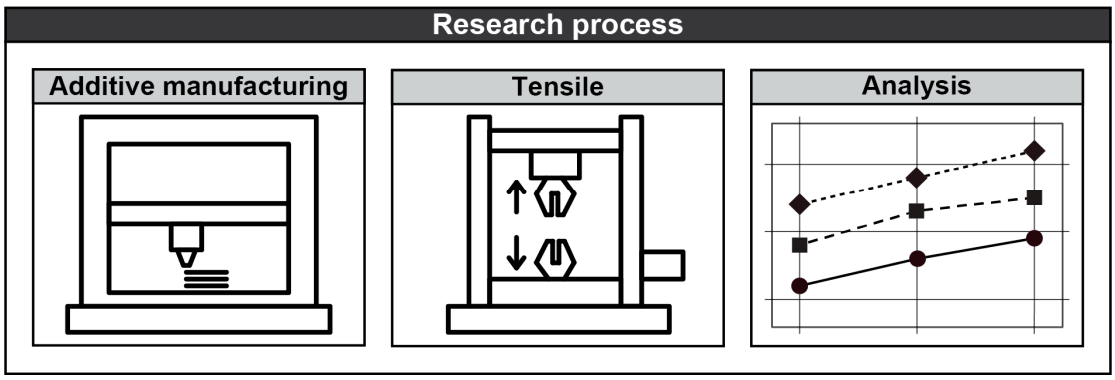

Figure 1. The flow of the experimental study: 3D printing, tensile and analysis of samples.

For the 3D creation of the control samples, the CreatBot™ D600 Pro 3D printer (Henan Creatbot Technology Limited, Zhengzhou, China) was used. The choice of this particular printer was made purposefully. First of all, the large printing volume it provides (0.216 m^3) allows the simultaneous printing of all samples, resulting in them being printed under the same conditions. In addition, the constant temperature that can be maintained inside, thanks to its casing, allows for even better printing results. Regarding the material chosen for the research, it is Recycled-PETG: EVO (NEEMA3D™, Athens, Greece). It consists of recycled polyethylene terephthalate (PETG) raw material, already used in industry, modified so that it becomes filament and can be printed again. It presents important properties such as high impact resistance and excellent flexibility and is almost warping free. In addition, it is a durable filament with high purity that allows for easy geometry printing. At the same time, it is worth noting that for the correct printing of the specific material and the protection of the nozzle from which it is extruded, it is advisable to use hardened steel material in the nozzle. The following table, Table 1, lists the properties of the specific material, according to its manufacturer [37].

Table 1. Recycled PETG yarn characteristics: EVO.

Description	Test Method	Typical Value
Specific gravity	ASTM D1505	1.25 g/cc
MFR 200 °C/5 kg	ISO 1183	7.5 g/10 min
Tensile strength at yield	ISO 527	46 MPa
Strain at break	ISO 527	61%
Tensile modulus	ISO 527	2050 MPa
Impact strength	ISO 527	5.9 kJ/m^2
Printing temp.	-	230–250 °C

Eighteen 3D-printed samples resulted from the combinations of the selected parameters for a comprehensive study. The variables set are percentage of infill, print speed and type of infill. More specifically,

- the percentage of infill refers to the completeness of the interior of a geometry and plays an important role in its strength, weight and structure. Its values range from 0% to 100% which is a complete compact structure.
- The print speed determines how slow or fast the printer motors will move in the X, Y, Z axes, as well as the nozzle ejection motor. Too low speeds can cause printing problems due to too little movement of the nozzle that ejects the material, and too high speeds can cause the material to fail to bond between layers. The measurement unit is mm/s.
- Finally, the type of infill refers to the infilling pattern of the interior of the structure. Its main purpose is to save time and printing material. It is not necessary for a part to be completely solid to be structurally sound. The kinds of patterns are many and some of them can improve the efficiency of the structure in strength, weight and printing life.

Table 2 lists the variables selected along with their corresponding values.

Table 2. The three variable parameters and their levels.

Infill (%)	Speed (mm/s)	Type
50	5	RectilinearField TianWiggle
70	20	
90	35	

The tensile testing of each experiment was performed on the Instron 3345 testing machine. More specifically, the total height of the tensile machine is 136 cm and its maximum force is 5 kN. Its grips can move at a maximum speed equal to 500 mm/min and

a minimum of 0.05 mm/min. Finally, measurements can be made in an area of 1123 mm vertically and 100 mm horizontally.

Figure 2 shows the main stages of the experimental study, the printing material, the definition of the parameters of the samples, the 3D printer to print the samples and the tensile force machine to check them.

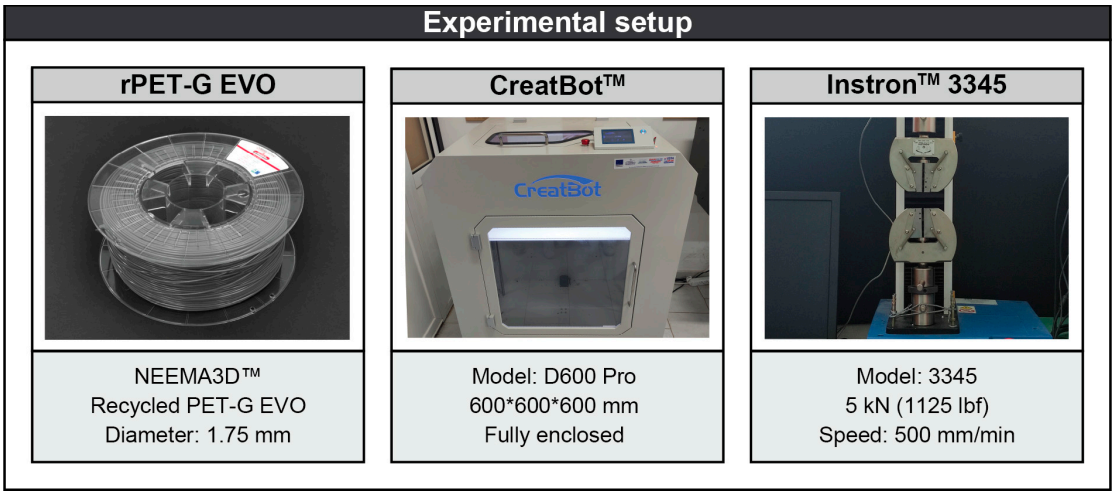

Figure 2. Printing filament, printing parameters, 3D printer and tensile machine.

Both nozzle and bed temperature were set to a constant value, as given by the manufacturer, that is, 240 °C and 60 °C, respectively. The nozzle cooling fan on each print was running at 100%. In addition, the diameter of the nozzle is 0.6 mm, while that of the thread is 1.75 mm. For the layer of the samples the value of 0.2 mm was chosen, with the result that 16 layers are needed to obtain the total height of the geometry. Also, the wall thickness around the geometry related to the number of parallel passages of the nozzle is defined by a natural number (N) and is directly related to the diameter of the nozzle. In this study, it is 2 × 0.6 mm = 1.2 mm. Finally, flow, that is, the flow rate that determines the amount of printing material that will pass through the nozzle, is expressed as a percentage and is equal to 100%. Table 3 lists all the constant parameters described above and used in the study.

Table 3. The fixed and common print settings.

Operation Parameter	Value
Nozzle Temperature	240 °C
Bed Temperature	60 °C
Filament Diameter	1.75 mm
Nozzle Diameter	0.6 mm
Layer	0.2 mm
Flow	100%
Cooling Fan	100%

Having defined the variable and non-variable parameters of 3D printing, the appropriate test specimen model was also selected. The ASTM D638 t1 standard, with a thickness of 3.2 mm, is suitable for corresponding measurements. Its overall dimensions are 165 mm × 19 mm × 3.2 mm, while its critical area is 57 mm × 13 mm × 3.2 mm. It is worth noting that the forces required to break the specimens were smaller than the maximum force (5 kN) of the selected Instron 3345 tensile machine. In Figure 3 below is the model designed in two-dimensional form along with its main dimensions [38].

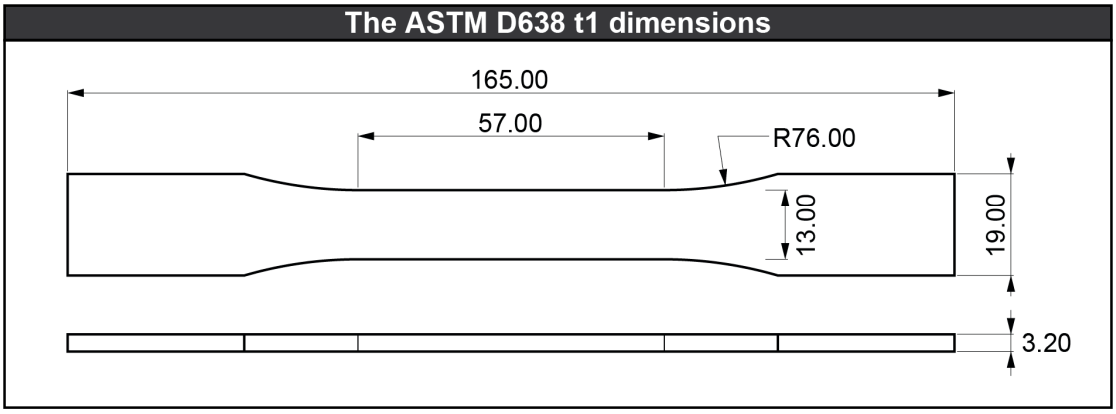

Figure 3. The selected template for tensile testing.

3. Results

3.1. Three-Dimensional Printing and Tensile Strength Measurement

In this section of the study, the results from the printouts and control measurements of the test pieces were gathered. In order to have more accuracy in the results, each sample was printed twice, yielding a total number of 36 specimens. The two resulting groups, A and B, were each printed in their entirety in order to have the same printing and environmental conditions. The samples were filed in the order they were printed and the corresponding group to which they belonged. To test their strength in the tensile machine, the tests were performed in pairs in sequence, starting from A1-B1, continuing with A2-B2 and ending in A18-B18. This sequence was chosen to simultaneously control for any intertrial drift errors. In the cases where the value of the deviation was large, another print was made of the specific samples, group C, for a better result. Figure 4 shows the main phases of the study, the printing of the samples, their tensile testing and the results after that.

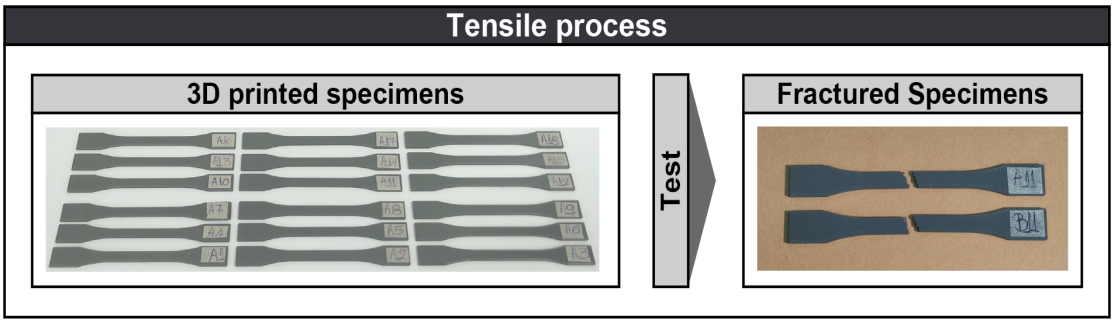

Figure 4. Three-dimensionally printed samples and testing their tensile strength.

Therefore, the 18 test combinations were generated through the three variables and their parameter levels. For their more complete organization, the following table was created. In Table 4, the results of all the measurements performed in series are listed. In each test, the values of the variable parameters (the percentage of infill, the printing speed, the type of infill), as well as the average tensile force required respectively in kilonewtons (kN), are reported separately in columns. Additionally, with the average force required to break each specimen, its corresponding stress in the last column was calculated, with a unit of measurement in megapascals (MPa). More specifically, to calculate the stress of each sample through the formula $\sigma = kN/A$, it is sufficient to take into account the force required to break the sample and area A of the critical area ($13 \times 3.2 = 41.6$ mm^2).

Table 4. Classification of the results from the experiments.

Test	Infill (%)	Speed (mm/s)	Type	Average Max Load (kN)	σ (MPa)
1	50	5	Rectilinear	1.043	25.06
2	50	20	Rectilinear	1.095	26.31
3	50	35	Rectilinear	1.139	27.38
4	70	5	Rectilinear	1.306	31.39
5	70	20	Rectilinear	1.383	33.25
6	70	35	Rectilinear	1.415	34.00
7	90	5	Rectilinear	1.632	39.22
8	90	20	Rectilinear	1.657	39.83
9	90	35	Rectilinear	1.654	39.75
10	50	5	Wiggle	1.355	32.57
11	50	20	Wiggle	1.438	34.56
12	50	35	Wiggle	1.455	34.96
13	70	5	Wiggle	1.671	40.17
14	70	20	Wiggle	1.752	42.12
15	70	35	Wiggle	1.739	41.79
16	90	5	Wiggle	1.906	45.82
17	90	20	Wiggle	1.946	46.77
18	90	35	Wiggle	1.876	45.08

Table 5 below presents the maximum tensile stress values for PETG and recycled PETG (r-PETG) materials. The research has identified the maximum tensile stresses for the specific materials in order to highlight, firstly, the already sufficient literature on PETG and, secondly, the limited research on recycled PETG, which is under study.

Table 5. The findings of the maximum stress levels, according to different studies and filaments.

Source	Max Stress (MPa)	Authors	References
PETG	41.58–48.04	Dolzyk and Jung	[39]
PETG	36.7	Bhahdari et al.	[40]
PETG	44.9	Franciszczak et al.	[41]
r-PETG	46.6	Bremer et al.	[13]

3.2. Interactions Plot Diagrams

The next step of the study was to gather the results from the measurements. A total of six interaction diagrams were obtained. Their purpose is to display each variable parameter in relation to the other two, in terms of the generated tensile strength. Looking at the six charts below, the following general facts emerge:

- Figure 5a illustrates the interaction of infill rate and speed. The tensile strength increases as the infill percentage increases. As for the tensile strength increase based on the speed, it is very small between the speed values. It is even observed that as the percentage of infilling increases to 90% and the speed approaches 35 mm/s, the tensile strength starts to drop in relation to the values of 5 mm/s and 20 mm/s.
- Figure 5b illustrates the interaction of infill rate and pattern type. The diagram proves that the type of infill plays a very important role in increasing the tensile strength, in combination with the percentage of infill. During the infill transition from 70% to 90% for the wiggle type, the largest tensile strength increase is observed.
- Figure 5c shows the interaction between speed and infill rate. Similarly to Figure 5a, it is observed that the increase in speed does not greatly affect the increase in tensile strength at each infill percentage.
- Figure 5d shows the interaction of speed and pattern type. The generated tensile strength varies in close values between the same type. Its lowest values are presented at the speed of 5 mm/s, but there is no significant difference at the other two speeds.
- Figure 5e illustrates the interaction of type of infill and percentage of infilling. The slope of the lines is upward for all three values. Therefore, the wiggle type shows a

greater trend in all percentages of infilling, compared to the rectilinear type, with the best at 90% infilling.

- Finally, Figure 5f illustrates the interaction between type of infill and speed. The results of the graph are similar to those of Figure 5d. The tensile strength in each pattern type has almost the same value, proving again that speed does not strongly affect the tensile strength levels.

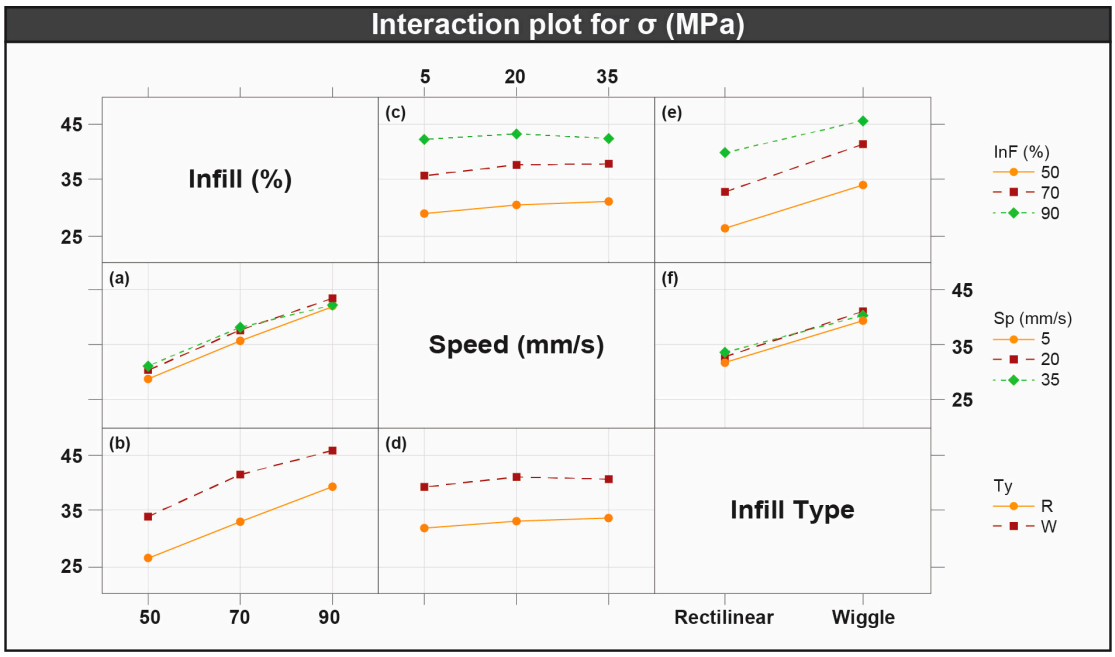

Figure 5. Diagram for the interactions between the three parameters: infill, speed and infill type.

Through Figure 5, some conclusions emerge:

- The percentage of infill strongly affected the strength of the specimens. In Figure 5a,b we observe the trend of the lines. The strength of the specimens increased as the percentage of infill increased. Increasing the speed values, as shown in Figure 5a, did not affect the lines. On the contrary, in Figure 5b the trend of the lines proves the strong influence of the infilling rate.
- The speed parameter increases the tensile strength mainly at the value of 20, as opposed to the other two values, 5 and 35. This is shown in Figure 5c,d. The increase in tensile strength does not have a linear shape, as the values decrease from 20–35.
- The type of infill chosen plays an important role in the durability of the 3D-printed specimen. The wiggle type compared to the rectilinear type requires a higher stress to destroy the structure. As can be seen in Figure 5e,f, by changing the values of the variable parameters infill rate and speed, the slope of the lines for the two values of the type also changes. In Figure 5e, for example, keeping the infilling rate constant at 50%, the stress difference between wiggle and rectilinear is 13.35 MPa, while keeping the infilling rate constant at 90%, the stress difference between wiggle and rectilinear is 11.84 MPa.
- According to the above, the parameter that significantly determines the trend of the samples, directly or indirectly, is the infill. The minimum tensile strength value of 25.06 MPa was recorded in test number 1. The variable parameters of this test are infill = 50%, velocity = 5 mm/s, infill type = rectilinear. In contrast, the maximum tensile strength value of 46.77 MPa was observed/recorded in test number 17. The variable parameters of this test are infill = 90%, velocity = 20 mm/s, infill type = wiggle.

3.3. Definition of the Regression Equation

In the continuation of the research, the experimental results were used to develop a prediction model. The second order polynomial regression (PE) was defined, described by Equation (1). The non-linearity of Equation (1) results in the requirement of linear, quadratic and cross terms. This equation is formulated below:

$$\sigma = -13.76 + 0.649 \times InF + 0.3534 \times Sp + 1.061 \times Ty - 0.001693 \times InF^2 - 0.00313 \times Sp^2 - 0.002048 \times InF \times Sp - 0.00373 \times InF \times Ty - 0.00242 \times Sp \times Ty \quad (1)$$

where: σ = maximum tensile strength, InF = percentage of infill, Sp = speed, Ty = type of infill.

Using the above Equation (1), it is possible to predict the maximum tensile strength for each combination of variable parameters. It is worth noting, however, that for this specific calculation, the values of the variable parameters must be between the limits that have been set. More specifically, the values that can be selected for the variable parameter infill must range between 50% and 90%. Accordingly, for the speed variable parameter, they must be 5 mm/s to 35 mm/s. The infill type variable parameter can be either rectilinear or wiggle. For example, the sample can be constructed with values of 65% infill, 25 mm/s speed and the wiggle type of infill. In order to test the performance of the mathematical model and the contribution rates of the terms to the response, an analysis of variance (ANOVA) was performed. This analysis used a confidence level of 95%. Table 5 below shows the ANOVA results. Considering the R-sq(pred) = 97.72% and *p*-value = 0.000 of the developed model, they can contribute to the high accuracy for the calculated ultimate tensile strength model.

According to Table 6, the term with a *p*-value greater than 0.05 is the term Sp × Ty, meaning that it is non-significant in terms of statistical significance. At the same time, the variable that enhances the produced tensile strength is the type of infill, with a percentage of 44.77%. Accordingly, the remaining infill% and speed with rates of 24.67% and 13.22% have a notable effect. The contribution of the InF × Sp term is 5.89%. Finally, the terms with the smallest contribution to the model are InF × Ty, InF^2, Sp^2 with their percentages reaching 3.24%, 3.58% and 3.86%.

Table 6. Analysis of variance results.

Source	Degree of Freedom	Sum of Squares	Mean Square	f-Value	*p*-Value	Contribution %
Regression	8	746.064	93.2580	226.21	0.000	
Error	9	3.710	0.4123			
Total	17	749.774				
	R-sq = 99.51%	R-sq(adj) = 99.07%		R-sq(pred) = 97.72%		
Term						
InF (%)	1	12.660	12.6600	30.71	0.000	24.67
Sp (mm/s)	1	6.782	6.7822	16.45	0.003	13.22
Ty	1	22.972	22.9724	55.72	0.000	44.77
InF^2	1	1.834	1.8338	4.45	0.064	3.58
Sp^2	1	1.983	1.9832	4.81	0.056	3.86
InF × Sp	1	3.021	3.0207	7.33	0.024	5.89
InF × Ty	1	1.666	1.6659	4.04	0.075	3.24
Sp × Ty	1	0.394	0.3944	0.96	0.354	0.77

3.4. Residual Analysis Graphs and Relative Error

Figure 6 shows the residual analysis (1), residual vs. fit (2) and residual vs. order graphs. The distribution followed by the residuals is shown in graph (1) to be normal. Additionally, in (2) and (3) it is shown that no systematic error occurred in the procedure followed.

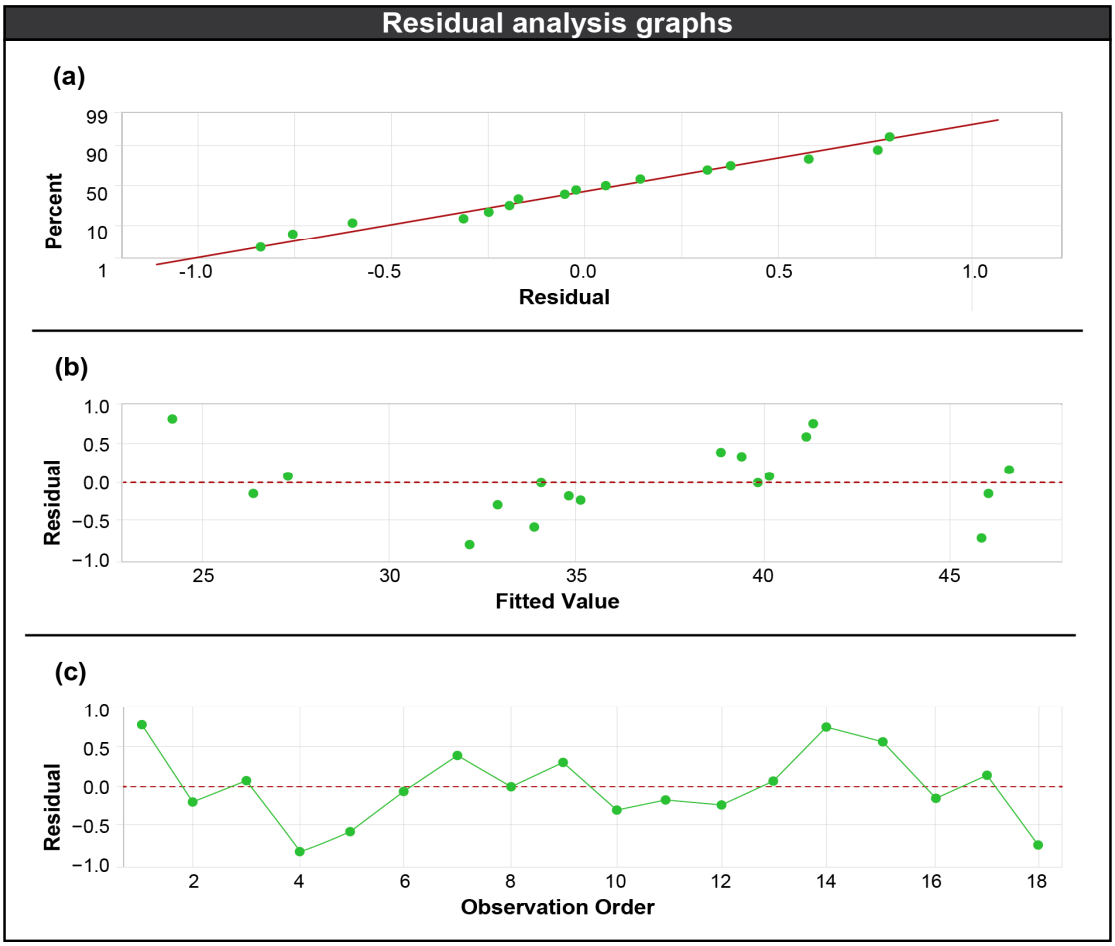

Figure 6. Residual analysis and model summary. The residual analysis (**a**), residual vs. fit (**b**) and residual vs. order graphs (**c**).

Below, Figure 7 shows the graph with the absolute relative error (%) between the actual results of each test and the predicted values obtained by mathematical model. The error values range between 0.01% and 3.20%, which proves that the final mathematical model is accurate.

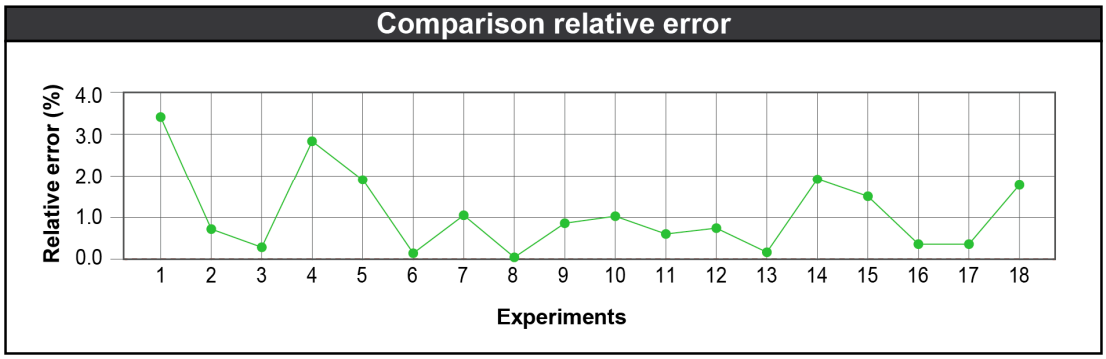

Figure 7. The relative error between real and model results.

3.5. Three-Dimensional Surface Plots

In addition to two-dimensional graphs that depict relationships between parameters, there are also three-dimensional surface plots. In particular, the trend obtained through the measurements is illustrated in relation to two of the parameters set during the printing

of the 3D-printed samples. Some variables are the percentage of infill, which refers to the fullness of the interior of a geometry and affects its weight, strength and structure, the print speed, which determines the movement of the printer motors in the three main axes, and the type of infill refers to the infilling pattern of the interior of the structure, affecting strength and weight efficiency. At the same time, the stress is the output of the results for the 3D-printed geometry, with measurement in MPa. The higher its value, the better the mechanical properties presented by the recycled PETG material.

Figure 8a shows the relationship between the speed (Sp) and infill rate (InF) parameters along with their combined effect on tensile strength. As the infill percentage increases from 50% to 90%, the tensile strength values increase accordingly. Therefore, the greater the percentage of infilling contained inside the geometry, the better its mechanical strength. Increasing the speed, especially to the value of 20, can help to extrude the material better, enhancing the results. However, the variations seen in the chart between values of 5 and 35 are small. Therefore, no particular effect is observed on the increase in the mechanical properties of the 3D-printed sample due to the speed but there is thanks to the infill rate parameter.

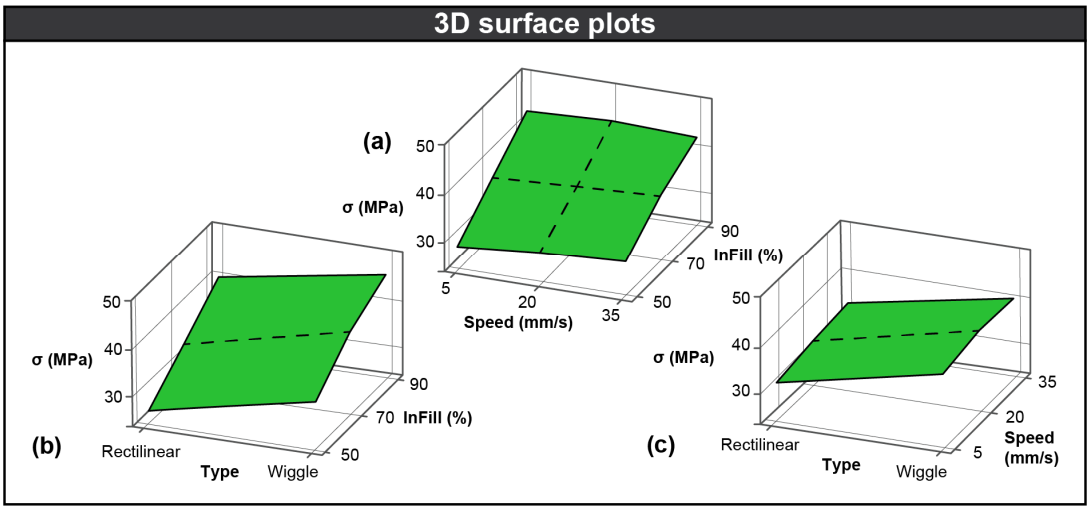

Figure 8. Three-dimensional surface plots with the stress relationship produced by the combination: speed vs. infill (**a**), type vs. infill (**b**) and type vs. speed (**c**).

Figure 8b shows the combined effect of the pattern type (Ty) and infill rate (InF) parameters, along with the generated tensile strength. Accordingly, in this diagram it is observed that the increase in material content inside the structure results in the strengthening of the sample. The tensile strength value increases more strongly when the infilling percentage reaches 90%. In addition, the sample becomes stronger in terms of its mechanical strength when wiggle is chosen as the type of infilling. Therefore, the strong tensile strength increase is highly influenced first by the type of infilling and then by the percentage of infilling, which improves the performance of the 3D-printed sample.

Finally, Figure 8c shows the relationship of the generated tensile strength with the combination of the pattern type (Ty) and speed (Sp) parameters. It is observed that as the type of infilling changes, a linear increase in tensile strength occurs. On the other hand, it is not the same, since printing at 20 mm/s gives the highest tensile strength value, and then it starts to decrease when reaching 35 mm/s. This suggests that the best interlayer material deposition occurs with the medium velocity value. In summary, the 3D graph shows that choosing the right type of fill and an intermediate value of velocity creates a strong 3D section, with type of infill playing the determining role versus velocity.

4. Conclusions

This study presents an investigation on the effects of three fabrication parameters on the generated tensile strength of 3D-printed specimens. The fabrication material of the samples used is a recycled-PETG polymer. The 3D samples were printed on the Creat-BotTM D600 Pro FFF class 3D printer. The three parameters concerning the settings of the 3D printing are the infill rate, the speed and the type of infill. Eighteen different experimental trials resulted from the implementation of a full factorial design, with all possible combinations of the structural features. At the same time, in order to inprove the reliability of the experiments, each specimen was printed twice. Finally, the mathematical model for each combination of values was defined through the aggregation and processing of the total stress results collected from the tensile test. Below, the conclusions obtained through the results and observations of the experiments are presented:

- Increasing the infill rate parameter greatly increases the strength of the 3D-printed sample. At the same time, the changes in the type of the infill inside the structure directly affect the slope of the lines separately for each level value.
- Increasing the speed parameter did not particularly increase the tensile strength of the specimens. Increasing tensile strength does not create a linear pattern. The higher the percentage of filling inside the structure, the higher the increase in tensile strength.
- The type of infill chosen plays an important role in the strength of the 3D-printed specimen. The second type (wiggle) compared to the first type (rectilinear) requires a higher stress to destroy the structure. The slope of the lines for the two type values changes, as do the values of the infill rate and speed variables.
- The parameter that significantly determines the trend of the samples, directly or indirectly, is the infill.
- The maximum tensile strength value, 46.77 MPa, was observed in test number 17 (infill = 90%, velocity = 20 mm/s, infill type = wiggle).
- The minimum tensile strength value, 25.06 MPa, was recorded in test number 1 (infill = 50%, velocity = 5 mm/s, infill type = rectilinear).

Author Contributions: Conceptualization, L.F. and N.E.; methodology, L.F.; software, L.F.; validation, L.F., P.K. and N.E.; formal analysis, L.F. and P.K.; investigation, L.F. and A.T.; resources, L.F. and N.E.; data curation, L.F., A.T. and N.E.; writing—original draft preparation, L.F., A.T., P.K. and N.E.; writing—review and editing, L.F., A.T., P.K. and N.E.; visualization, L.F., A.T. and N.E.; supervision, A.T. and N.E.; project administration, A.T. and N.E.; funding acquisition, L.F. and N.E. All authors have read and agreed to the published version of the manuscript.

Funding: This research received no external funding.

Institutional Review Board Statement: Not applicable.

Informed Consent Statement: Not applicable.

Data Availability Statement: The original contributions presented in this study are included in the article. Further inquiries can be directed to the corresponding author(s).

Conflicts of Interest: The authors declare no conflicts of interest.

References

1. Tzotzis, A.; Manavis, A.; Efkolidis, N.; García-Hernández, C.; Kyratsis, P. Analysis of the Influence of Structural Characteristics on the Tensile Properties of Fused Filament Fabricated ABS Polymer Using Central Composite Design. *Appl. Mech.* **2023**, *5*, 20–35. [CrossRef]
2. Mishra, A.; Jatti, V.S.; Sefene, E.M.; Paliwal, S. Explainable Artificial intelligence (XAI) and supervised machine learning-based algorithms for prediction of surface roughness of additively manufactured polylactic acid (PLA) specimens. *Appl. Mech.* **2023**, *4*, 668–698. [CrossRef]
3. Wang, J.; Yang, B.; Lin, X.; Gao, L.; Liu, T.; Lu, Y.; Wang, R. Research of TPU materials for 3D printing aiming at non-pneumatic tires by FDM method. *Polymers* **2020**, *12*, 2492. [CrossRef] [PubMed]
4. Anderson, I. Mechanical properties of specimes 3D printed with virgin and recycled polylactic acid. *3D Print. Addit. Manuf.* **2017**, *4*, 110–115. [CrossRef]

5. Kumar, R.; Singh, R.; Farina, I. On the 3D printing of recycled ABS, PLA and HIPS thermoplastics for structural applications. *PSU Res. Rev.* **2018**, *2*, 115–137. [CrossRef]
6. Atakok, G.; Kam, M.; Koc, H.B. Tensile, three-point bending and impact strength of 3D printed parts using PLA and recycled PLA filaments: A statistical investigation. *J. Mater. Res. Technol.* **2022**, *18*, 1542–1554. [CrossRef]
7. Bergaliyeva, S.; Sales, D.L.; Delgado, F.J.; Bolegenova, S.; Molina, S.I. Manufacture and characterization of polylactic acid filaments recycled from real waste for 3D printing. *Polymers* **2023**, *15*, 2165. [CrossRef]
8. Aberoumand, M.; Soltanmohammadi, K.; Soleyman, E.; Rahmatabadi, D.; Ghasemi, I.; Baniassadi, M.; Abrinia, K.; Baghani, M. A comprehensive experimental investigation on 4D printing of PET-G under bending. *J. Mater. Res. Technol.* **2022**, *18*, 2552–2569. [CrossRef]
9. Quintana, R.; Choi, J.W.; Puebla, K.; Wicker, R. Effects of build orientation on tensile strength for stereolithography-manufactured ASTM D-638 type I specimens. *Int. J. Adv. Manuf. Technol.* **2010**, *46*, 201–215. [CrossRef]
10. Özen, A.; Auhl, D.; Völlmecke, C.; Kiendl, J.; Abali, B.E. Optimization of manufacturing parameters and tensile specimen geometry for fused deposition modeling (FDM) 3D-printed PETG. *Materials* **2021**, *14*, 2556. [CrossRef]
11. Hanon, M.M.; Marczis, R.; Zsidai, L. Anisotropy evaluation of different raster directions, spatial orientations, and fill percentage of 3D printed PETG tensile test specimens. *Key Eng. Mater.* **2019**, *821*, 167–173. [CrossRef]
12. Abid, S.; Messadi, R.; Hassine, T.; Ben Daly, H.; Soulestin, J.; Lacrampe, M.F. Optimization of mechanical properties of printed acrylonitrile butadiene styrene using RSM design. *Int. J. Adv. Manuf. Technol.* **2019**, *100*, 1363–1372. [CrossRef]
13. Bremer, M.; Janoschek, L.; Kaschta, D.; Schneider, N.; Wahl, M. Influence of plastic recycling—A feasibility study for additive manufacturing using glycol modified polyethylene terephthalate (PETG). *SN Appl. Sci.* **2022**, *4*, 156. [CrossRef]
14. Zander, N.E.; Gillan, M.; Lambeth, R.H. Recycled polyethylene terephthalate as a new FFF feedstock material. *Addit. Manuf.* **2018**, *21*, 174–182. [CrossRef]
15. Pozo-Antonio, J.S.; Noya-Pintos, D.; Sanmartín, P. Moving toward Smart Cities: Evaluation of the Self-Cleaning Properties of Si-Based Consolidants Containing Nanocrystalline TiO_2 Activated by Either UV-A or UV-B Radiation. *Polymers* **2020**, *12*, 2577. [CrossRef]
16. Seno Flores, J.D.; de Assis Augusto, T.; Lopes Vieira Cunha, D.A.; Gonçalves Beatrice, C.A.; Henrique Backes, E.; Costa, L.C. Sustainable polymer reclamation: Recycling poly (ethylene terephthalate) glycol (PETG) for 3D printing applications. *J. Mater. Sci. Mater. Eng.* **2024**, *19*, 16. [CrossRef]
17. Vidakis, N.; Petousis, M.; Tzounis, L.; Maniadi, A.; Velidakis, E.; Mountakis, N.; Papageorgiou, D.; Liebscher, M.; Mechtcherine, V. Sustainable additive manufacturing: Mechanical response of polypropylene over multiple recycling processes. *Sustainability* **2020**, *13*, 159. [CrossRef]
18. Lehrer, J.; Scanlon, M.R. The development of a sustainable technology for 3D printing using recycled materials. In Proceedings of the 2017 Mid-Atlantic Section Fall Conference, Reading, PA, USA, 6–7 October 2017.
19. Hou, X.; Sitthisang, S.; Song, B.; Xu, X.; Johnson, W.; Tan, Y.; Yodmuang, S.; He, C. Entropically Toughened Robust Biodegradable Polymer Blends and Composites for Bone Tissue Engineering. *ACS Apllied Mater. Interfaces* **2024**, *16*, 2912–2920. [CrossRef]
20. Olawumi, M.A.; Oladapo, B.I.; Olugbade, T.O. Evaluating the impact of recycling on polymer of 3D printing for energy and material sustainability. *Resour. Conserv. Recycl.* **2024**, *209*, 107769. [CrossRef]
21. Latko-Durałek, P.; Dydek, K.; Boczkowska, A. Thermal, rheological and mechanical properties of PETG/rPETG blends. *J. Polym. Environ.* **2019**, *27*, 2600–2606. [CrossRef]
22. Ramírez-Revilla, S.; Camacho-Valencia, D.; Gonzales-Condori, E.G.; Márquez, G. Evaluation and comparison of the degradability and compressive and tensile properties of 3D printing polymeric materials: PLA, PETG, PC, and ASA. *MRS Commun.* **2023**, *13*, 55–62. [CrossRef]
23. Sepahi, M.T.; Abusalma, H.; Jovanovic, V.; Eisazadeh, H. Mechanical properties of 3D-printed parts made of polyethylene terephthalate glycol. *J. Mater. Eng. Perform.* **2021**, *30*, 6851–6861. [CrossRef]
24. Mercado–Colmenero, J.M.; Martin–Doñate, C. A novel geometric predictive algorithm for assessing compressive elastic modulus in MEX additive processes, based on part nonlinearities and layers stiffness, validated with PETG and PLA materials. *Polym. Test.* **2024**, *133*, 108389. [CrossRef]
25. Hsueh, M.H.; Lai, C.J.; Wang, S.H.; Zeng, Y.S.; Hsieh, C.H.; Pan, C.Y.; Huang, W.C. Effect of printing parameters on the thermal and mechanical properties of 3d-printed pla and petg, using fused deposition modeling. *Polymers* **2021**, *13*, 1758. [CrossRef] [PubMed]
26. Kumar, R.; Sharma, H.; Saran, C.; Tripathy, T.S.; Sangwan, K.S.; Herrmann, C. A comparative study on the life cycle assessment of a 3D printed product with PLA, ABS & PETG materials. *Procedia CIRP* **2022**, *107*, 15–20.
27. Kováčová, M.; Kozakovičová, J.; Procházka, M.; Janigová, I.; Vysopal, M.; Černičková, I.; Krajčovič, J.; Špitalský, Z. Novel hybrid PETG composites for 3D printing. *Appl. Sci.* **2020**, *10*, 3062. [CrossRef]
28. Singh, A.K.; Bedi, R.; Kaith, B.S. Composite materials based on recycled polyethylene terephthalate and their properties—A comprehensive review. *Compos. Part B Eng.* **2021**, *219*, 108928. [CrossRef]
29. Oussai, A.; Bártfai, Z.; Kátai, L. Development of 3D printing raw materials from plastic waste. A case study on recycled polyethylene terephthalate. *Appl. Sci.* **2021**, *11*, 7338. [CrossRef]
30. Bex, G.J.; Ingenhut, B.L.; Ten Cate, T.; Sezen, M.; Ozkoc, G. Sustainable approach to produce 3D-printed continuous carbon fiber composites:"A comparison of virgin and recycled PETG". *Polym. Compos.* **2021**, *42*, 4253–4264. [CrossRef]

31. Srinidhi, M.S.; Soundararajan, R.; Satishkumar, K.S.; Suresh, S. Enhancing the FDM infill pattern outcomes of mechanical behavior for as-built and annealed PETG and CFPETG composites parts. *Mater. Today Proc.* **2021**, *45*, 7208–7212. [CrossRef]
32. Kasmi, S.; Ginoux, G.; Allaoui, S.; Alix, S. Investigation of 3D printing strategy on the mechanical performance of coextruded continuous carbon fiber reinforced PETG. *J. Appl. Polym. Sci.* **2021**, *138*, 50955. [CrossRef]
33. Woern, A.L.; Byard, D.J.; Oakley, R.B.; Fiedler, M.J.; Snabes, S.L.; Pearce, J.M. Fused particle fabrication 3-D printing. *Materials* **2018**, *11*, 1413. [CrossRef] [PubMed]
34. Tzotzis, A.; Antoniadis, A.; Kyratsis, P. Multivariate modelling of AA6082-T6 drilling performance using RSM, ANN and response optimization. *Int. J. Lightweight Mater. Manuf.* **2024**, *7*, 531–545. [CrossRef]
35. Tzotzis, A.; Garcia-Hernandez, C.; Huertas-Talon, J.L.; Kyratsis, P. 3D FE Modelling of Machining Forces during AISI 4140 Hard Turning. *J. Mech. Eng./Stroj. Vestn.* **2020**, *66*, 467. [CrossRef]
36. Tzotzis, A.; García-Hernández, C.; Huertas-Talón, J.L.; Kyratsis, P. Influence of the nose radius on the machining forces induced during AISI-4140 hard turning: A CAD-based and 3D FEM approach. *Micromachines* **2020**, *11*, 798. [CrossRef]
37. NEEMA3D™ r-PETG: EVO. Available online: http://www.neema3d.com/neema3dt-evo-sign-materials/recycled-petg-evo (accessed on 28 November 2024).
38. *ASTM D638-22*; Standard Test Method for Tensile Properties of Plastics. American Society for Testing and Materials: West Conshohocken, PA, USA, 2022. Available online: https://www.astm.org/d0638-22.html (accessed on 28 November 2024).
39. Dolzyk, G.; Jung, S. Tensile and Fatigue Analysis of 3D-Printed Polyethylene Terephthalate Glycol. J Fail. *Anal. Preven* **2019**, *19*, 511–518. [CrossRef]
40. Bhandari, S.; Lopez-Anido, R.; Gardner, D. Enhancing the interlayer tensile strength of 3D printed short carbon fiber reinforced PETG and PLA composites via annealing. *Addit. Manuf.* **2019**, *30*, 100922. [CrossRef]
41. Franciszczak, P.; Piesowicz, E.; Kalnins, K. Manufacturing and properties of r-PETG/PET fibre composite—Novel approach for recycling of PETG plastic scrap into engineering compound for injection moulding. *Compos. Part B Eng.* **2018**, *154*, 430–438. [CrossRef]